Hetero-/homogeneous combustion of premixed hydrogen-oxygen mixture in a micro-reactor with catalyst segmentation

Qingbo Lu, Jianfeng Pan *, Song Hu, Aikung Tang, Xia Shao

(School of Energy and Power Engineering, Jiangsu University, Zhenjiang 212013, P.R. China)

*Corresponding author: Dr. Jianfeng Pan

Address: School of Energy and Power Engineering, Jiangsu University, 301 Xuefu Road, Zhenjiang 212013, PR China

Tel.: +86-0511-88780210

Fax: +86-0511-88780216

E-mail address: mike@ujs.edu.cn

ABSTRACT

Numerical simulations with detailed homogeneous (gas phase) and heterogeneous (catalytic) chemistries of premixed hydrogen-oxygen mixture were performed inside a rectangular micro-combustor. The effects of catalytic walls on the homogeneous combustion were investigated via varying catalyst segment layouts and sizes. The interactions between heterogeneous and homogeneous reactions were discussed. It was shown that the heterogeneous reactions become weak when the catalyst disposition is shifted toward the outlet along the streamwise. The homogeneous combustion also becomes obviously weakened downstream behind the catalyst segmentation, except the exit. Moreover, with increasing catalyst segment size, the hydrogen conversion ratio increases and the mean outlet temperature reduces. The competition of the fresh fuel between the heterogeneous and homogeneous reactions result in the inhibition of heterogeneous reactions on homogeneous combustion. In summary, the heterogeneous reactions can obviously improve the combustion efficiency in a micro catalytic combustor. As expected, the effects of catalytic walls were more pronounced for the micro combustor systems.

Keywords: Heterogeneous and homogeneous combustion; Hydrogen; Catalyst segmentation; Numerical simulation; Micro-reactor

1. Introduction

Micro-scale combustors for micro-power generation and micro-propulsion systems have received increasing attention due to their many distinct advantages such as high energy density, low manufacturing cost and environmental friendly, compared with conventional chemical batteries [1,2]. However, it is worth noting that the characteristic scale of micro-combustors ranges from a few millimeters to sub-millimeters, which results in an unstable homogeneous combustion inside the

micro-combustor. It is well accepted that there are three primary aspects to generate flame extinction in a micro-combustor, which are high surface-to-volume ratio, thermal quenching and radical quenching on the wall, respectively. The surface-to-volume ratio of micro-combustors is far larger than that of the macro scale combustor, which leads to enhanced heat loss to the surroundings. The heat and radical generated from the reactions also depletes fast on the wall, resulting in the extinction of the homogeneous combustion [1-5]. Conventional flame stability and fuel conversion efficiency can be greatly reduced via controlling these influencing factors in a micro-combustor. In order to solve these problems and extend the stable operating range of a micro scale combustor, many useful strategies were proposed, such as use heat-recirculating combustors to reduce heat losses [4,5], utilizing quenching resistant fuel and employing catalytic combustors to enhance reaction and suppress radical depletion on the wall [6-8]. In practice, the catalytic combustion was used for improving combustion stability, which was considered as one of the best available methods. Surface catalytic (heterogeneous) reactions often have lower activation energies than pure gaseous (homogeneous) reactions, and allow sustaining chemical reactions at lower temperature and possess higher heat losses, resulting in lower probability of thermal quenching.

In the catalytic micro-combustor, the catalytic layers are deposited on the combustor walls, and the effect of that can suppress the intrinsic flame instabilities of micro- and meso-scale channels. Many scholars [8-10] have studied the effects of various parameters on the flame stability in the catalytic micro-combustor used by computational fluid dynamics (CFD) simulations or experimental methods, such as equivalence ratio, inlet velocity, wall material, heat loss, blow out behavior and combustor dimension. Maruta et al. [8] numerically studied the extinction limits in a micro-catalytic channel with multi-step reactions. Their research showed that, for adiabatic walls, the equivalence ratio at the

extinction limit monotonically decreases with an increasing Reynolds number. However, for non-adiabatic conditions, the extinction curve exhibits a U-shaped dual-limit behavior due to the heat loss and insufficient residence time compared to chemical time. Benedetto et al. [9] reported the effects of cross-sectional geometry on the ignition/extinction behavior of catalytic micro-combustors by three-dimensional CFD simulations, and built the stability maps. Appel et al. [10,11] investigated the numerical and experimental model of catalytic reactions used to stabilize the combustion reactions in micro-channels for H_2-air mixture over platinum (Pt). The understanding of the heterogeneous and homogeneous reaction kinetics is crucial to the development of such systems.

It has been shown that the catalytic wall plays an important role in heterogeneous and homogeneous reactions. Fanaee and Esfahani [12,13] conducted an analysis on effects of the catalytic wall and channel hydraulic diameter on the combustion process in a micro combustor. The results show that the catalytic walls can extend the flammability limits of a lean reactive mixture more than a rich one. Also, they confirmed that using the catalytic wall can decrease the quenching distance in meso and micro scale reactors as compared to the non-catalytic wall case. Chen et al. [14] demonstrated that the catalytic wall has its sustaining and competing effects on homogeneous combustion in a micro tube. In another numerical research conducted by Chen et al. [15], they showed that the existence of catalyst segmentation promotes the performance and conversion ratio of the micro reactor by improving homogeneous combustion. Smyth et al. [16,17] experimentally investigated the surface oxidation on small-scale catalytic coupons of Pt foil for methane/air and propane/air mixtures. The surface reactions can be divided into three phases along the plate. It is suggested that the design of small-scale reactors should proceed by exploiting the intense reaction of phases I (close to the leading edge) and phase II (surface temperature plateaued at a high value) through boundary layer interruption.

It is imperative that the complex heterogeneous-homogeneous interactions should be further studied. There are many interactions between heterogeneous and homogeneous reaction under certain specific factors. It is demonstrated that the heterogeneous reaction can promote the flame combustion due to the catalytically induced exothermicity. It has the inhibition for homogeneous reactions caused by the competition of reactants between the catalytic reaction and homogeneous reaction. Wang et al. [18] investigated the comparison of reaction intensity between catalytic and non-catalytic combustors. The results show that the catalytic combustor displays a high stability and weak reaction intensity. In addition, the experimental data shows that the catalytic combustion can effectively improve the homogenous combustion efficiency in a catalytic micro-reactor [19]. Zade et al. [20] also numerically investigated the importance of gas-phase and surface reactions for H_2/air mixture in planar micro-channels. The results show that lean limitations of the gas-phase reactions become negligible when compared to surface reactions [10]. However, the interactions between homogeneous and heterogeneous reaction are still not clearly understood in the catalytic micro combustor.

In our previous related work [21,22], CFD simulations and related experiments were performed on hetero-/homogeneous combustion of premixed hydrogen-oxygen mixtures inside a sub-millimeter planar combustor with a rectangular channel. The main parameters, such as wall materials, inlet velocity, equivalence ratio and combustor dimensions, have the crucial effects on the combustion characteristics. In this work, we study the effects of catalytic walls described by different sizes and layouts of catalyst on the combustion characteristics. A three-dimensional simulation model was performed to analyze the multi-steps homogeneous and heterogeneous chemistries for premixed hydrogen-oxygen mixture in the special micro combustor coated with a catalyst. Furthermore, an investigation will be carried out to explore the hetero-/homogeneous combustion phenomenon in a

micro-combustor by numerical simulations with variable reaction mechanisms.

2. Numerical model and model validation

2.1 Computing models and boundary conditions

A three-dimensional simulation is performed on the micro combustor to simulate the reactive gas flow and reaction characteristics, using the CFD code FLUENT [23]. The rectangular channel has 10 mm in length (- *x*, L), 10 mm in width (- *y*, W), and 1 mm in height (- *z*, H). Thickness of the wall of the combustor is 0.4 mm as shown in Fig.1. In the CFD modeling, the platinum catalyst at different locations are coated on the inner silicon carbide (SiC) wall. The laminar finite rate model is employed due to the low inlet flow velocity. The mass governing equations are discretized by a first-order upwind scheme in the numerical model, including steady-state Navier–Stokes equations, mass and energy conservation equations, and chemical radical equation, respectively. SIMPLE algorithm is chosen to deal with the pressure-velocity coupling. The boundary conditions are as follows. The velocity-inlet and out-flow are specified at the inlet and outlet, respectively. The hydrogen-oxygen equivalence ratio is 1.0, and the inflow velocity is 2 m/s which is close to the flame speed of hydrogen. On each wall, a no-slip boundary condition is imposed. The initial temperature for the chamber solid wall, the incoming mixture temperature and the surrounding temperature of the chamber are all specified as 300K. The combustor is completely exposed in ambient air and heat loss of the exterior wall is convected by air.

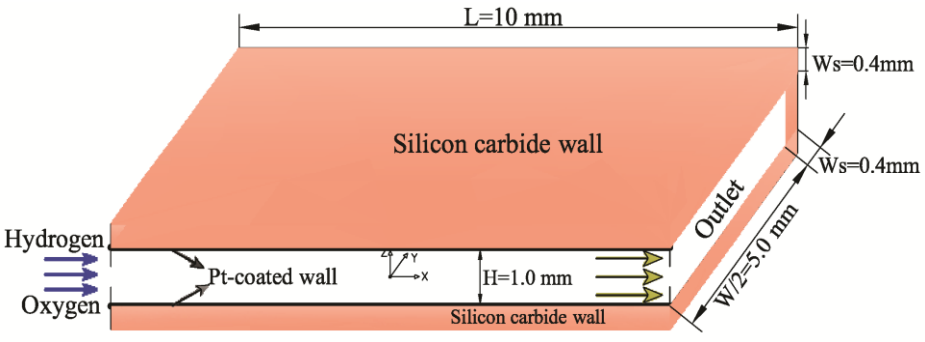

Fig.1. Schematic of the computational domain.

In the computation model, an optimized uniform structured grid with 140400 cells is employed, as shown in Fig.2. The fined grids are utilized in the action region near the wall for obtaining high-resolution boundary data and analyzing surface layer catalysis chemistry in the computational domain. The simulation convergence is declared when the residuals of all governing equations approached steady states. The convergent criterions of all residuals in this work are set to be less than 10^{-6}.

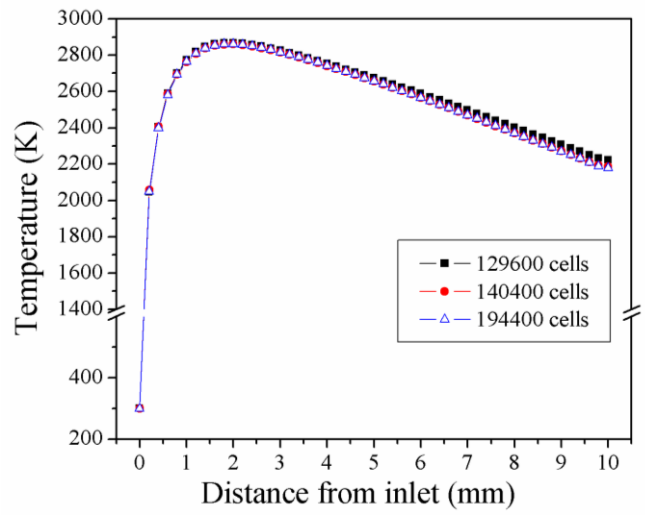

Fig.2. Centerline temperature profiles of combustor at different mesh densities.

A skeletal gas phase reaction mechanism proposed by Miller and Bowman for hydrogen-oxygen mixture is used in the computation model, which has 9 species and 19 reversible elementary reactions [24]. The surface chemistry mechanism for hydrogen over platinum is taken from Deutschmann et al [25]. This simulation includes five surface species: Pt(s), H(s), H_2O(s), OH(s) and O(s).

2.2 Validation of the computational model

In order to validate the numerical model and chemical mechanisms used in the study, we compare between the results from numerical simulation and experiment. The experimental setup is given in a previous study by Pan et al. [5]. The temperature distribution in the combustion chamber is measured by an infrared thermal imager (Camera model: Thermovision TM A40) and recorded by a personal

computer. The infrared thermal imager is capable of measuring a maximum temperature of 2000 ℃ with an accuracy of ±2%. Fig. 3(a) shows the comparison in outer wall temperature distribution patterns from experiment and simulation using the catalytic combustor with 2 mm length of catalyst segmentation. Fig. 3(b) shows the centerline temperature profiles on the outer wall of the combustor from experiment and simulation with non-/catalyst. The same initial conditions are used: a volumetric flow rate of hydrogen of 600 mL/min and equivalence ratio of 1.0. There is good agreement between simulations and experimental results. The maximum deviation between simulations and experiment results are 3.0% (with catalytic wall), 2.8% (with 2 mm length of catalyst segmentation) and 1.9% (with non-catalytic wall), respectively.

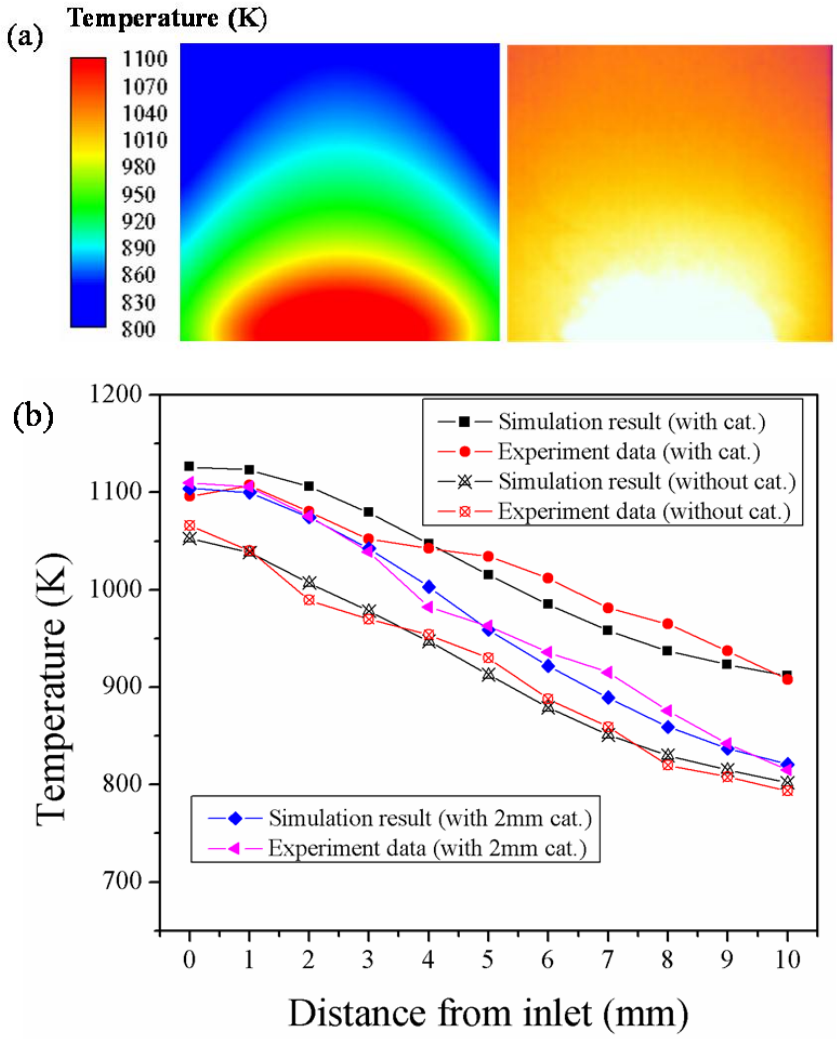

Fig.3. Experimental validation of computational model.(a) Comparison in the outer wall temperature of combustor from simulation and experiment with 2 mm length of catalyst segmentation, (left: simulation; right: experiment), (b) Comparison of centerline temperature profiles on the outer wall of the combustor from experiment and simulation with non-/catalytic wall.

3. Results and discussion

3.1 Combustion characteristics for different reaction models

To understand the interactions between heterogeneous and homogeneous reactions of hydrogen-oxygen mixture in the micro-combustor, and to examine the performances of the combustor, three combinations of multi-steps gas phase and catalytic reaction mechanisms are employed to clearly identify homo-/heterogeneous reactions by CFD simulation in rectangular channel. Three modes with the same initial conditions in this section are the homogeneous reaction mode (Case A), the coupled homogeneous and heterogeneous reactions mode (Case B) and the heterogeneous reactions mode (Case C), respectively. Specifically, when the inner wall is coated with the catalyst, a heterogeneous reaction occurs. On the contrary, when the inner wall is not coated with the catalyst, a homogenous reaction occurs.

Fig. 4 shows the computed contours of the temperature and OH concentration distributions in the micro-combustor for three cases. The simulation results of the homogeneous reaction mode shows that the highest temperature occurs in the fluid region, and the high temperature zone displays a cone shape, as shown in Fig. 4(a). The temperature distributions for the coupled homogeneous and heterogeneous reactions mode are depicted in Fig. 4(b), indicating that the shape of high temperature region is similar to that of Case A. In addition, the significantly decreasing of the maximum temperature of gaseous mixture and the high temperature region are shown as compared to Case A, due to the suppression of

heterogeneous reactions. For the Case C in Fig. 4 (c), it can be found that the highest temperature only occurs on the inner wall, and the temperature distribution exists in the channel near the catalytic wall due to the heat transformation from the wall to the fluid region.

The OH concentration distribution can be used to verify whether homogeneous combustion occurred inside the micro-combustor. The high OH concentration can be used to mark the reaction zone and high temperature regions [15]. Fig.4 (d, e, f) show the computed contours of OH concentration in the micro-combustor for three cases. The shape of high OH concentration region is similar to the corresponding high temperature region. It is shown in Fig.4 (d) that the highest OH concentration exists near the inner wall. Fig.4 (e) shows that maximum OH concentration level of Case B near the inner wall clearly decreases when compared to Case A, due to the presence of heterogeneous reactions. Meanwhile, the reactants for homogeneous reaction decrease, and then the OH concentration decrease in the channel. The OH species is normally absorbed on the catalyst surface and regarded as a reactant in the heterogeneous reactions. Moreover, this also results in the reduced high OH concentration region as compared to Case A. Fig.4 (f) shows the computed contour of OH concentration for the Case C. The high OH concentration region occurs near the catalytic surface and the maximum value of OH concentration is sustained at a low level. The region of high OH concentration clearly suggests that heterogeneous reactions take place on the catalytic wall.

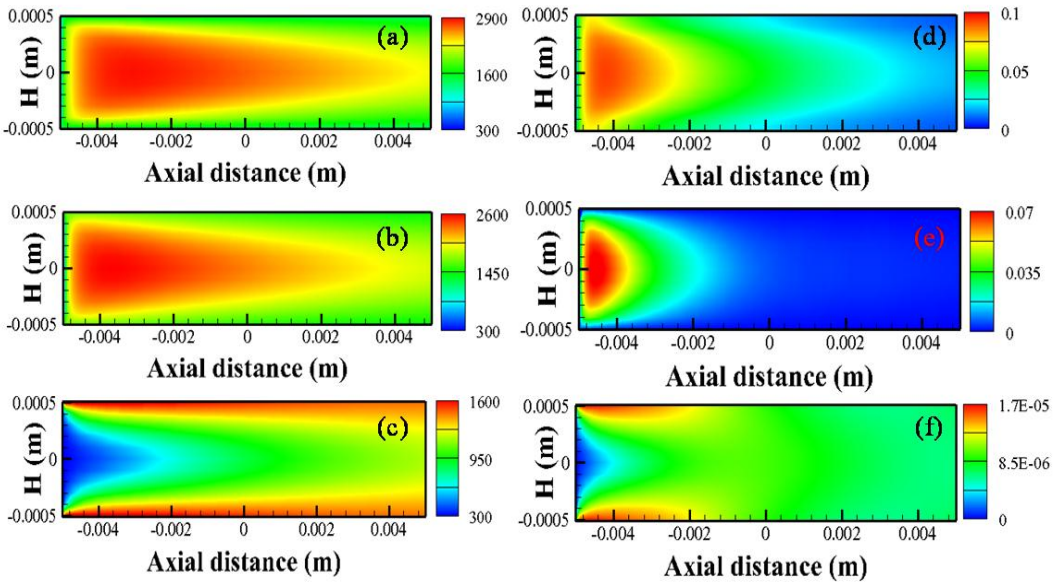

Fig.4.Computed contours of temperature and OH concentration in the center section of micro combustor (y=0) for three cases: (a, d) the Case A, (b, e) the Case B, (c, f) the Case C.

In order to more clearly identify the reaction characteristics of these cases, Fig.5 shows the temperature, OH and H_2 mass fraction profiles of the centerline of the flow channel and inner upper wall. The temperature increases in the combustor due to the heat released by reactions. The centerline temperature profiles of the flow channel along the streamwise display a distinct difference, as shown in Fig.5 (a). It can be seen that the temperature first increases and then decreases with increasing distance from the inlet for Case A and Case B. Nevertheless, in Case C, the temperature always increases with increasing distance from inlet, indicating that the heat was released by heterogeneous reaction and transferred from the surface wall to the fluid region by convection. The homogeneous combustion usually occurs in the fluid region, but the heterogeneous reaction only takes place on the inner wall. From the centerline temperature profiles of the upper inner wall along the streamwise, it can be seen that the temperature first increases and then decreases with increasing distance from inlet. Furthermore, the maximum temperatures in Case B and Case C are lower than that of Case A due to the presence of heterogeneous reactions. While the heterogeneous reactions exist, the profiles of temperature

distributions on the inner wall are consistent at the position from entrance to 4 mm, but the rest of temperature spots for Case B are always higher than that of Case C. In this regard, the heat is first released by heterogeneous reactions on the catalytic wall and then lost by convection on the outer wall surface. Meanwhile, the heat is transferred from the flow region to the surface wall due to the presence of higher temperature in the flow channel sides. This therefore leads to the existence of higher temperature spots for Case B at the place from 4 mm to the exit.

Fig.5 (b) shows the OH concentration profiles along the streamwise on centerline of channel and inner upper wall. The OH concentration first sharply increases and then decreases from inlet to exit. The maximum value of OH concentration in Case C is thousand times less than that in Case A. The peak value of OH species concentrations is at 0.5mm. It is obvious that the peak value of OH species concentrations shifts towards inlet when compared to Case A. This is due to the inhibition of heterogeneous reaction on the homogeneous combustion. For the OH concentration along the centerline of inner wall, the results show that the OH concentration in Case B is obviously lower than that of Case A because the OH species was absorbed by catalyst. Fig.5 (c) shows the H_2 mass fraction profiles, indicating that the fuel consumption for the three cases decreases from the inlet to the exit. From the results of Case A and Case B, the H_2 mass fraction both sharply decreases, but the fuel consumption significantly increases in Case B as compared to Case A because the reactants are consumed in the homogeneous reactions and heterogeneous reactions. Therefore, it is further demonstrated that the reactants have a competitive relationship between the heterogeneous reaction and the homogeneous reaction in Case B.

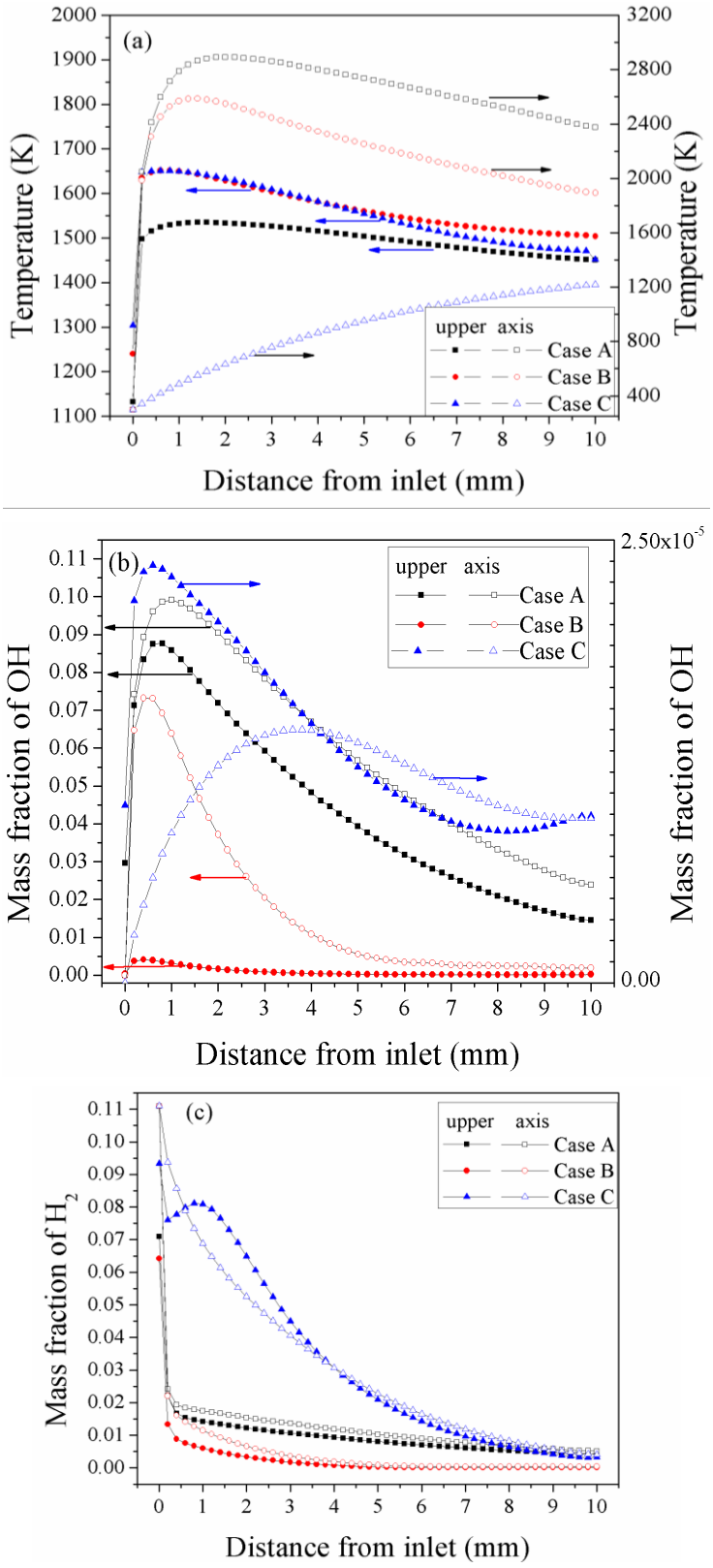

Fig.5. Temperature, OH mass fraction and H_2 mass fraction profiles along the centerline of the flow channel and inner upper wall, (a) temperature profiles, (b) OH mass fraction profiles, (c) H_2 mass fraction profiles.

3.2 Effect of catalyst segmentation

3.2.1 Effect of catalyst segment layout

For the coupled homogeneous and heterogeneous reactions mode, it is important to further explore the interactions between homogeneous and heterogeneous reactions. The effects of the catalytic walls on homogeneous reactions can be observed under various catalyst layouts. In this work, the upper inner wall is divided into ten segments in the combustor. The catalyst segmentation is 1 mm long (Lc) and located at the entrance from 0 to 1mm along the streamwise. Thus it can be marked X = 0 at entrance, and the other catalyst segments are also marked by this method. In this paper, six catalyst segmentswere investigated under the same initial condition, which are X = 0, 1, 2, 4, 7, 9, respectively.

Fig. 6 shows the mass fraction of OH species with non-/catalyst along the streamwise on the centerline of the inner wall and the fluid region. For the X= 0, it can be seen in Fig. 6 (a) that the OH concentration slowly increases and is then maintained invariably from the entrance to 1mm (the length of catalyst segmentation). This region is dominated by heterogeneous reactions, and as such, the OH concentration rapidly increases and then slowly reduces with increasing distance from 1 mm. It can also be seen that the OH concentration is significantly lower than that of a non-catalyst case behind catalytic zone. The OH concentration in Fig. 6 (b) rapidly increases as it approaches the entrance and then slowly decreases, but the corresponding value in catalyst case is much lower compared with non-catalyst case. For the X= 1, 2, 4, 7, the OH concentration on the centerline of the inner wall or in the fluid region rapidly reduces and is then maintained near the catalyst segmentation. Furthermore, the OH concentration is significantly lower than that in the adjacent position with non-catalytic zone due to a strong adsorption of catalyst to OH species, resulting in a low concentration area on the catalytic surface. However, for the X=9, the distribution of OH concentration has no obvious change as

compared to a non-catalyst case. Therefore, in the catalytic zone, it can be implied that the reactants and free radicals participated in catalytic reaction are drained, indicating a lower concentration. These results clearly show that the heterogeneous reactions have a major impact on homogeneous combustion near catalyst segmentation except at the exit, and have a significant effect on the downstream behind catalytic zone. In particular, when the catalyst segmentation is placed at the entrance, it is most influential. Hence, it can be concluded that the homogeneous combustion are suppressed by heterogeneous reactions in the coupled homogeneous and heterogeneous reactions mode.

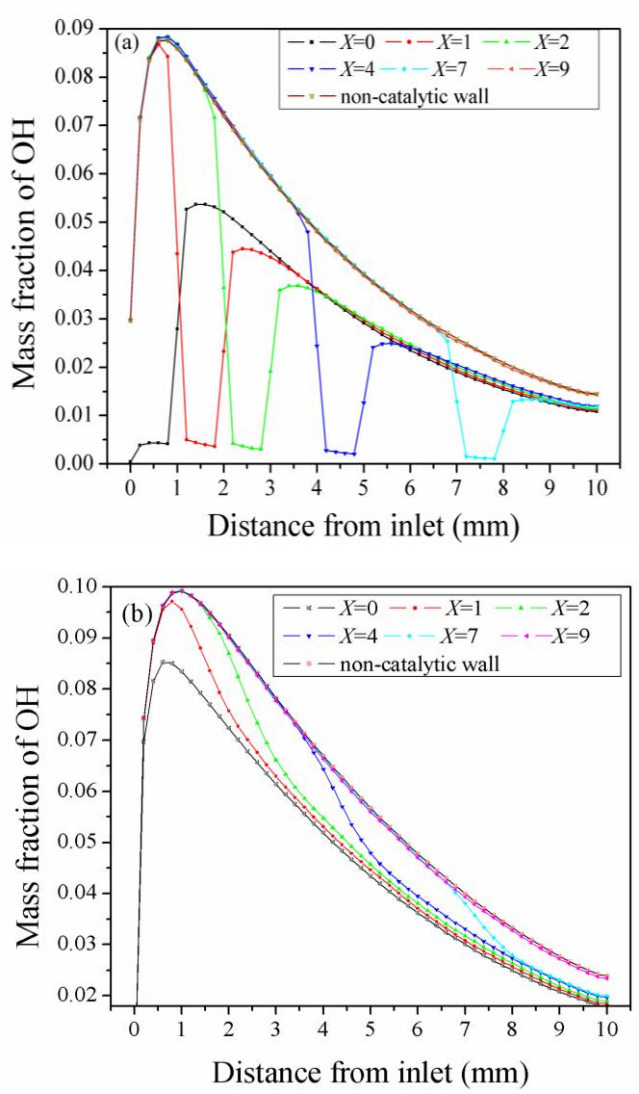

Fig.6. OH mass fraction profiles along the streamwise on the centerline of the inner wall (a) and fluid region (b).

It is well know that O, H species are absorbed by a catalyst, and H species is the first product in the hydrogen decomposition reaction and often used to identify the start of a reaction[15]. Fig. 7 shows the mass fraction of O, H species with non-/catalyst on the centerline of the inner wall. As can be seen from the above profiles of OH concentration, the distribution of O, H concentration displays a similar track. For the X= 0, 1, 2, 4, 7, the O, H concentrations are lower than those of the non-catalyst case at the same site of catalyst segmentation. In addition, the profiles of O, H concentrations show a distinct trough near the catalyst segmentation. There is a significant lowering behind the catalytic zone, when compared with non-/catalyst cases, except X= 9. The heterogeneous reactions occurred on the catalyst segmentation, have an important effect on the O, H concentration distributions at the downstream region, especially X= 0. The sticking coefficient of O, H species are both 1.0, it means that the O, H species has high absorption ability on the catalytic surface, thus resulting in the existence of low concentration region in the catalytic zone. Also, the part of the formed O, H species from the homogenous reaction can diffuse to the catalytic surface and initiate the absorption reactions, revealing that the heterogeneous reactions have the inhibition effect on the homogeneous combustion caused by the competition of intermediate between heterogeneous reaction and homogeneous reaction [15, 26]. Comparison of the non-catalyst case and the X= 9 case, the O, H concentration distributions have a similar trend. For the effect of heterogeneous reactions on homogenous combustion, it is greatest when the catalyst segmentation is placed at the inlet. With changing the positions of catalyst segmentation toward the exit, the effect is shown to weaken and fade away.

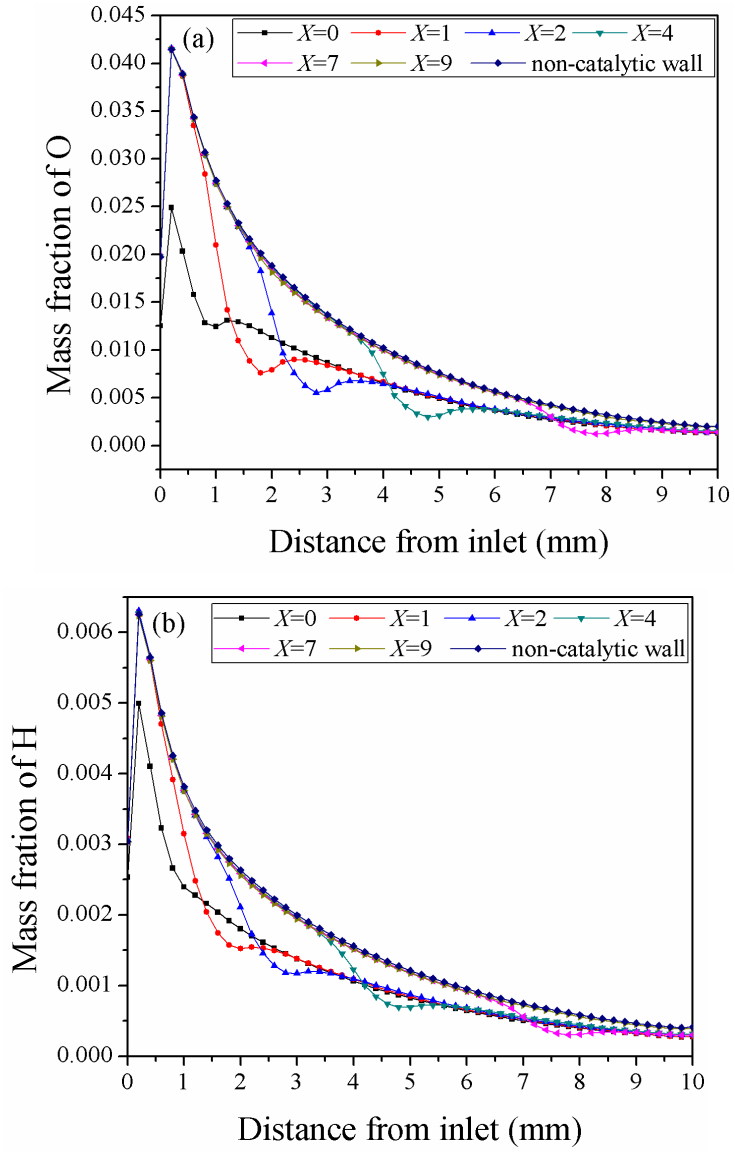

Fig.7. O, H mass fraction profiles on the upper wall along the streamwise, (a) O mass fraction profiles, (b) H mass fraction profiles.

Fig.8 shows H_2 mass fraction profiles under different positions of the catalyst segmentation on the centerline of the channel and inner upper wall. As shown in Fig.8 (a), the mass fraction of H_2 deceases along the streamwise on the centerline of the upper wall. The existence of grooves near the catalyst segmentation for X=0, 1, 2, 4, 7 are attributed to the consumed fuel in the heterogeneous reactions. This indicates the presence of a competition over the fuel between the heterogeneous and homogeneous reactions[26]. The heterogeneous reactions consume the reactants, resulting in decreasing of H_2

concentration on the centerline of the channel, as show in Fig.8 (b). Nevertheless, it can be seen from Fig.8 that the H_2 concentration decreases in downstream behind the catalyst segmentation compared with non-catalyst case, indicating an increase of hydrogen conversion ratio. Therefore, the combustion efficiency of combustor is improved by means of the catalysis.

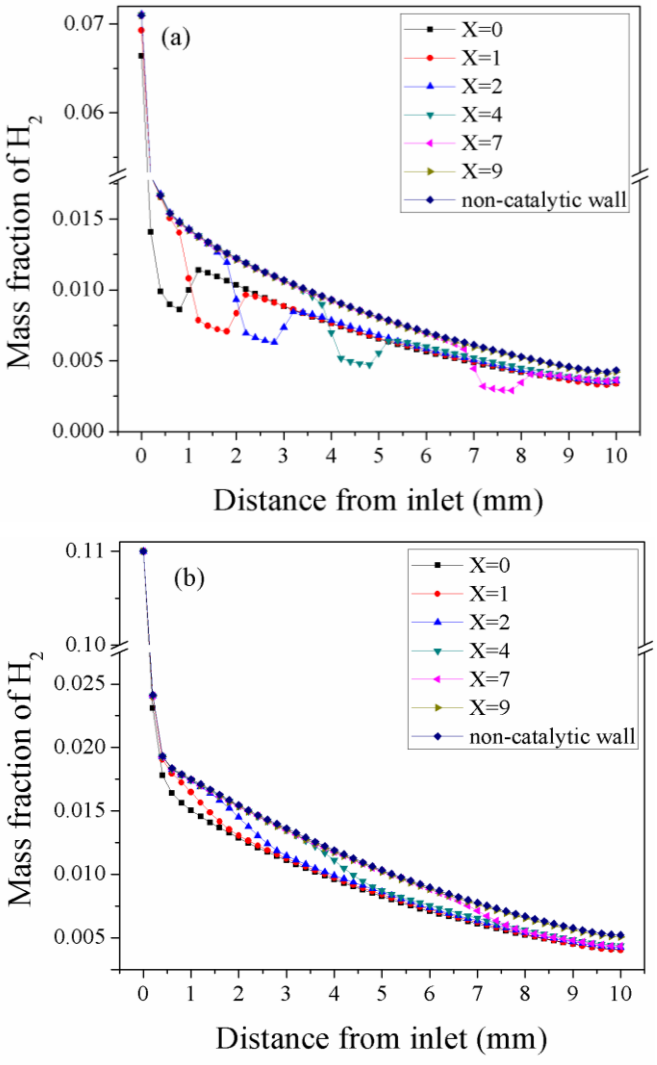

Fig.8. H_2 mass fraction profiles along the streamwise on the centerline of inner upper wall (a) and on the centerline of channel (b).

Fig.9 shows the mean outlet temperature under different positions of catalyst segmentation. It can be noted that the mean temperature increases gradually with the increase of the *X* value. The mean temperature is lowest when the catalyst segmentation is placed at the entrance, but the mean

temperature for the *X*=9 is highest. It is further illustrated that the catalyst segmentation under different positions has an effect on the homogeneous combustion. The influence of catalyst segment placed at the entrance is particularly the largest.

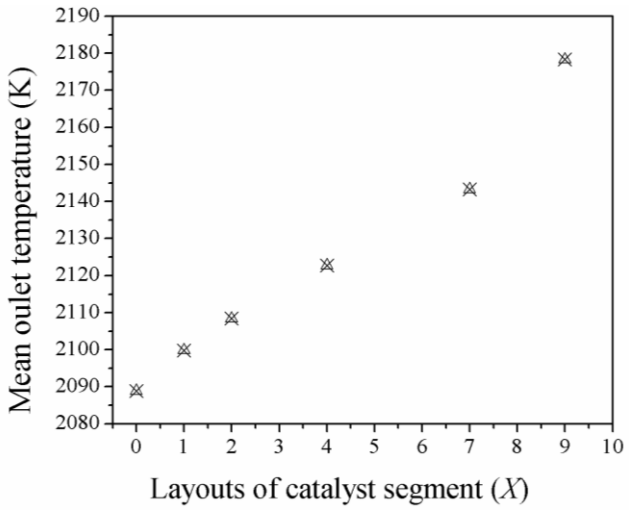

Fig.9. Profile of mean outlet temperature under different positions of catalyst segmentation.

3.2.2 Effect of catalyst segment size

In order to further examine the effects of catalytic walls on the combustor properties, different sizes of catalyst segmentation on the upper inner wall are applied in this work. The catalytic area ratio θ can be defined as the area of catalyst segmentation to the overall area of upper inner wall. The θ value can be given in the range of 0~1.0 when the area of catalyst segmentation is from 0 to 100 mm^2. Detailed computational results are investigated under θ=0, 0.1, 0.2, 0.4, 0.5, 0.6, 0.8, 1.0, which are based on the coupled homogeneous and heterogeneous reactions mode at the same boundary condition mentioned above.

Fig.10 shows the temperature and OH concentration profiles along the streamwise on the centerline of channel and inner upper wall respectively. As shown in Fig.10 (a), the centerline temperature in the channel sharply increases and then slowly decreases along the streamwise. The

temperature variation exists a significantly for every case, such as the θ=1.0 case, the outlet temperature on the centerline of flow channel is equal to 2048 K, which is decreased by 14% as compared to the θ=0 case, owing to the existence of heterogeneous reactions. It can be seen from Fig.10 (b) that the temperature of catalytic wall significantly increases at the upstream. The heat is released by the heterogeneous reactions on the catalytic wall, indicating a higher wall temperature. However, the released heat is transferred from the catalytic zone to the non-catalytic zone, resulting in gradually increasing the maximum wall temperature from θ=0 to θ=1 case. The heat is generated by the heterogeneous reaction on the catalytic wall, indicating a higher wall temperature, and the generated heat is also transferred from the catalytic zone to the non-catalytic zone. Furthermore, with increasing size of catalyst segmentation, the generated heat of heterogeneous reactions gradually improves up to steady states. Fig.10 (c) shows the OH concentration on the centerline of channel along the streamwise. The peak of OH concentration for the θ=0 case is placed at 1 mm, and the peak values for other cases are all placed at 0.5 mm. This suggests that homogeneous combustion shifts towards inlet attributed to increasing the size of catalytic zone. Once the OH species is absorbed in the heterogeneous reaction, the chain reaction of the homogeneous reactions is terminated. This shows that the homogeneous reactions are suppressed by heterogeneous reactions due to the OH species being one of the intermediate products of homogeneous combustion. Fig.10 (d) shows that OH concentration increases along the centerline of the upper wall. The data displays two slopes that stand for two different reaction zones. The first slope is smooth and the region is dominated by a heterogeneous reaction. Since OH species is absorbed by the catalyst, the OH concentration sharply decreases and maintains the low level near the catalytic zone. The other slope sharply increases due to no absorption reaction, and the homogeneous reaction plays an important role in the region. In addition, the level of OH concentration

decreases in the non-catalytic zone, when compared with the θ=0 case, caused by the absorption of catalyst in catalytic zone and the decreased amount of reactants for homogeneous combustion.

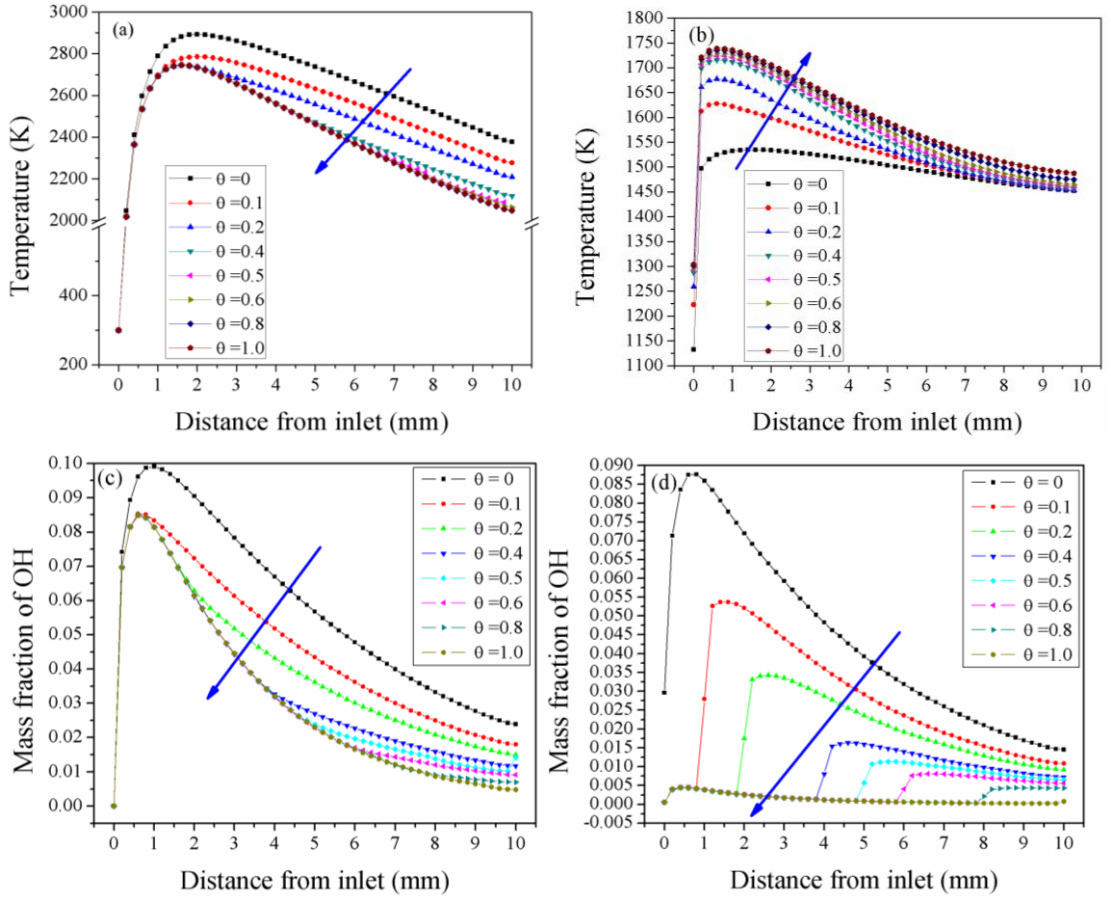

Fig.10. Temperature and OH concentration profiles along the streamwise under different catalytic area ratios: (a) temperature profiles on the centerline of channel, (b) temperature profiles on the centerline of the upper wall, (c) OH concentration profiles on the centerline of channel, (d) OH concentration profiles on the centerline of the upper wall.

During the multistep chemical process, the hydrogen conversion ratio is mainly considered as a key factor for combustion reaction, and the combustor properties are characterized by those different conversion ratios. Fig.11 shows the mean outlet temperature and hydrogen conversion ratio under different θ. It can be seen that the mean outlet temperature decreases when the catalytic area ratio increases. On the contrary, the hydrogen conversion ratio increases with increasing catalytic area ratio.

For θ=0 case, the highest mean outlet temperature and lowest hydrogen conversion ratio are observed. The residence time of gaseous species in the channel is so short that the combustion is incomplete. However, with increasing θ, the mean outlet temperature reduces and the hydrogen conversion ratio increases. For the θ=1 case, the hydrogen conversion ratio is enhanced by about 0.0331 compared with the θ=0 case. It is verified that the combustor performances can be significantly improved with the increase of the θ.

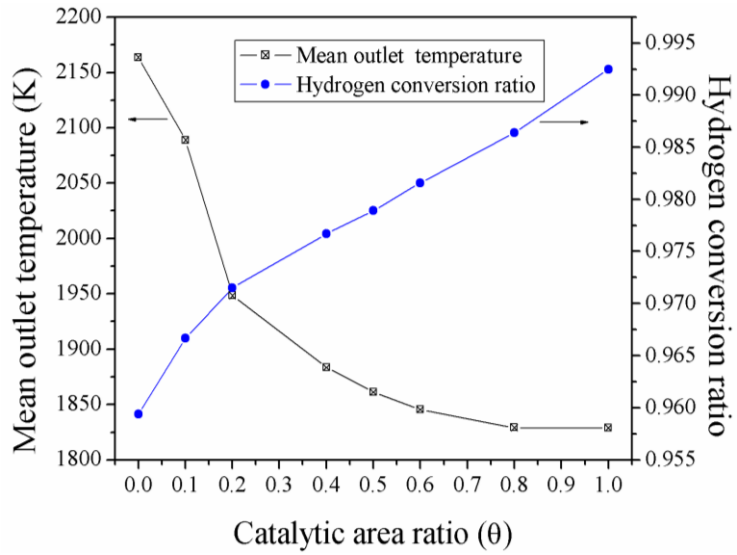

Fig.11. Profiles of mean outlet temperature and hydrogen conversion ratio under different catalytic area ratios.

4. Conclusions

Catalytic combustion is considered as an effective solution to improve combustion stability. In this work, the combustion characteristics for H_2/O_2 mixture over Pt surface were investigated by CFD numerical simulation with detailed heterogeneous and homogeneous mechanisms. In order to further reveal the effects of catalytic wall on homogeneous and heterogeneous combustion characteristics in the catalytic combustor, the layout and size of catalyst segmentation as influence factors were discussed. The following results were obtained from this study:

1.Three reaction characteristics are significantly different and investigated by numerical simulation with variable reaction mechanisms in the micro combustors. The existence of heterogeneous reaction has an inhibition effect on homogeneous reaction indicating that the decreasing of maximum temperature of the flame and the low OH concentration region. The promotion effect of heterogeneous reaction is displayed by enhancing hydrogen consumption.

2.The layout of catalyst segmentation plays an important role in the micro catalytic combustor systems. While the heterogeneous reactions is initiated on the catalytic wall, the radicals concentration in the downstream decreases because the radicals are absorbed at the catalytic zone. Meanwhile, the heterogeneous reactions are gradually weakened with shifting catalyst dispositions from inlet to outlet.

3.With the increase of the catalyst segment size, the hydrogen conversion ratio gradually increases and the mean outlet temperature decreases. This indicates that the occurrence of heterogeneous reactions can enhance the fuel conversion ratio and combustor performances. Therefore, the existence of the catalytic walls can improve the combustion efficiency for the micro catalytic combustor systems.

Acknowledgements

The authors wish to acknowledge the research grant from National Science Foundation of China (No. 51376082 and 51206066), Natural Science grant of Jiangsu province (No. BK20131253) and the Project Funded by the Priority Academic Program Development of Jiangsu Higher Education Institutions (PAPD).

References

[1] Chou S K, Yang W M, Chua K J, et al. Development of micro power generators–A review. Applied Energy, 2011, 88(1): 1–16.

[2] Ju Y, Maruta K. Microscale combustion: Technology development and fundamental research.

Progress in Energy and Combustion Science, 2011, 37(6): 669–715.

[3] Kaisare N S, Vlachos D G. A review on microcombustion: Fundamentals, devices and applications. Progress in Energy and Combustion Science, 2012, 38(3):321–359.

[4] Yang W M, Chou S K, Shu C, et al. Combustion in micro-cylindrical combustors with and without a backward facing step. Applied Thermal Engineering, 2002, 22(16): 1777–1787.

[5] Pan J F, Yang W M, Tang A K, et al. Micro combustion in sub-millimeter channels for novel modular thermophotovoltaic power generators. Journal of Micromechanics and Microengineering, 2010, 20(12):125021–125028.

[6] Maruta K. Micro and mesoscale combustion. Proceedings of the Combustion Institute, 2011, 33(1): 125–150.

[7] Yang W M, Chou S K, Shu C, et al. Study of catalytic combustion and its effect on microthermophotovoltaic power generators. Journal of Physics D: Applied Physics, 2005, 38(23): 42–52.

[8] Maruta K, Takeda K, Ahn J, et al. Extinction limits of catalytic combustion in microchannels. Proceedings of the Combustion Institute, 2002, 29(1):957–963.

[9] Benedetto A D, Sarli V D, Russo G. Effect of geometry on the thermal behavior of catalytic micro-combustors. Catalysis Today, 2010, 155:116–122.

[10] Appel C, Mantzaras J, Schaeren R, et al. An experimental and numerical investigation of homogeneous ignition in catalytically stabilized combustion of hydrogen/air mixtures over platinum. Combustion and Flame, 2002, 128(1):340–368.

[11] Appel C, Mantzaras J, Schaeren R, et al. Catalytic combustion of hydrogen air mixtures over platinum: validation of hetero/homogeneous chemical reaction schemes. Clean Air, 2004,5:21–44.

[12] Fanaee S A, Esfahani J A. Two-dimensional analytical model of flame characteristic in catalytic micro-combustors for a hydrogen–air mixture. International Journal of Hydrogen Energy, 2014, 39(9):4600–4610.

[13] Fanaee A, Esfahani J A. The Normalized Analysis of a Surface Heterogeneous Reaction of a Propane/Air Mixture into a Micro-Channel. Chinese Physics Letters, 2012, 29(12):124702–124706.

[14] Chen G B, Chen C P, Wu C Y, et al. Effects of catalytic walls on hydrogen/air combustion inside a micro-tube. Applied Catalysis A: General, 2007, 332(1):89–97.

[15] Chen G B, Chao Y C, Chen C P. Enhancement of hydrogen reaction in a micro-channel by catalyst segmentation. International Journal of Hydrogen Energy, 2008, 33(10):2586–2595.

[16] Smyth S A, Christensen K T, Kyritsis D C. Intermediate Reynolds number flat plate boundary layer flows over catalytic surfaces for “micro”-combustion applications. Proceedings of the Combustion Institute, 2009, 32(2):3035–3042.

[17] Smyth S A, Kyritsis D C. Experimental determination of the structure of catalytic micro-combustion flows over small-scale flat plates for methane and propane fuel. Combustion and Flame, 2012, 159(2):802–816.

[18] Wang Y, Zhou Z, Yang W, et al. Combustion of hydrogen-air in micro combustors with catalytic Pt layer. Energy Conversion and Management, 2010, 51(6): 1127–1133.

[19] Zhang Y, Zhou J, Yang W, et al. Effects of hydrogen addition on methane catalytic combustion in a micro tube. International Journal of Hydrogen Energy, 2007, 32(9): 1286–1293.

[20] Zade A Q, Renksizbulut M, Friedman J. Contribution of homogeneous reactions to hydrogen oxidation in catalytic microchannels. Combustion and Flame, 2012, 159(2): 784–792.

[21] Pan J F, Fan B W, Wu Q R, et al. Study on Catalytic Combustion of Premixed Hydrogen and

Oxygen in the Micro-scale. Journal of Mechanical Engineering. 2011, 47(24): 111–116.

[22] Pan J F, Wu Q R, Xue H, et al. Experimental Investigation of Catalytic Combustion in a Planar Micro Combustor[J]. Journal of Engineering Thermophysics, 2011, 32(8): 1430–1432.

[23] Fluent Inc. FLUENT User′s Guide. Lebanon, USA: Fluent Inc, 1999.

[24] Miller J A, Bowan C T. Mechanism and modeling of nitrogen chemistry in combustion. Progress in Energy and Combustion Science, 1989, 15(4): 287–338.

[25] Deutschmann O, Schmidt R, Behrendt F, et al. Numerical modeling of catalytic ignition, Twenty-Sixth Symposium (International) on Combustion, 1996: 1747–1754.

[26] Deutschmann O. Modeling of the Interactions Between Catalytic Surfaces and Gas-Phase. Catalysis Letters, 2015, 145(1):272-289.

Figure captions

Fig.1. Schematic of the computational domain.

Fig.2. Centerline temperature profiles of combustor at different mesh densities.

Fig.3. Experimental validation of computational model.(a) Comparison in the outer wall temperature of combustor from simulation and experiment with 2 mm length of catalyst segmentation, (left: simulation; right: experiment), (b) Comparison of centerline temperature profiles on the outer wall of the combustor from experiment and simulation with non-/catalytic wall.

Fig.4. Computed contours of temperature and OH concentration in the center section of micro combustor (y=0) for three cases: (a, d) the Case A, (b, e) the Case B, (c, f) the Case C.

Fig.5. Temperature, OH mass fraction and H_2 mass fraction profiles along the centerline of the flow channel and inner upper wall, (a) temperature profiles, (b) OH mass fraction profiles, (c) H_2 mass fraction profiles.

Fig.6. OH mass fraction profiles along the streamwise on the centerline of the inner wall (a) and fluid region (b).

Fig.7. O, H mass fraction profiles on the upper wall along the streamwise, (a) O mass fraction profiles, (b) H mass fraction profiles.

Fig.8. H_2 mass fraction profiles along the streamwise on the centerline of inner upper wall (a) and on the centerline of channel (b).

Fig.9. Profile of mean outlet temperature under different positions of catalyst segmentation.

Fig.10. Temperature and OH concentration profiles along the streamwise under different catalytic area ratios: (a) temperature profiles on the centerline of channel, (b) temperature profiles on the centerline of the upper wall, (c) OH concentration profiles on the centerline of channel, (d) OH concentration profiles on the centerline of the upper wall.

Fig.11. Profiles of mean outlet temperature and hydrogen conversion ratio under different catalytic area ratios.

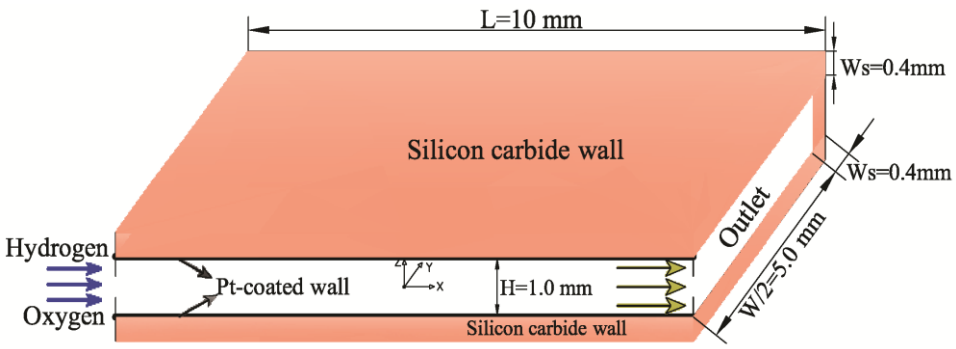

Fig.1. Schematic of the computational domain.

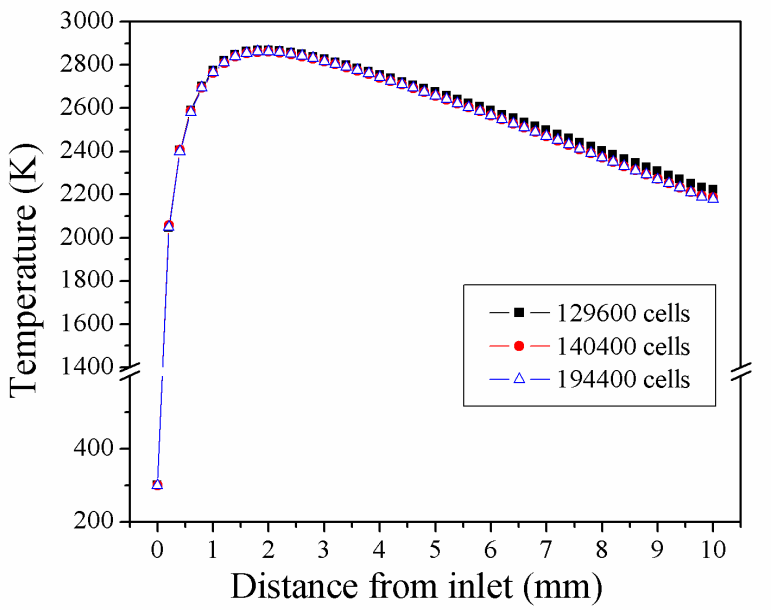

Fig.2. Centerline temperature profiles of combustor at different mesh densities.

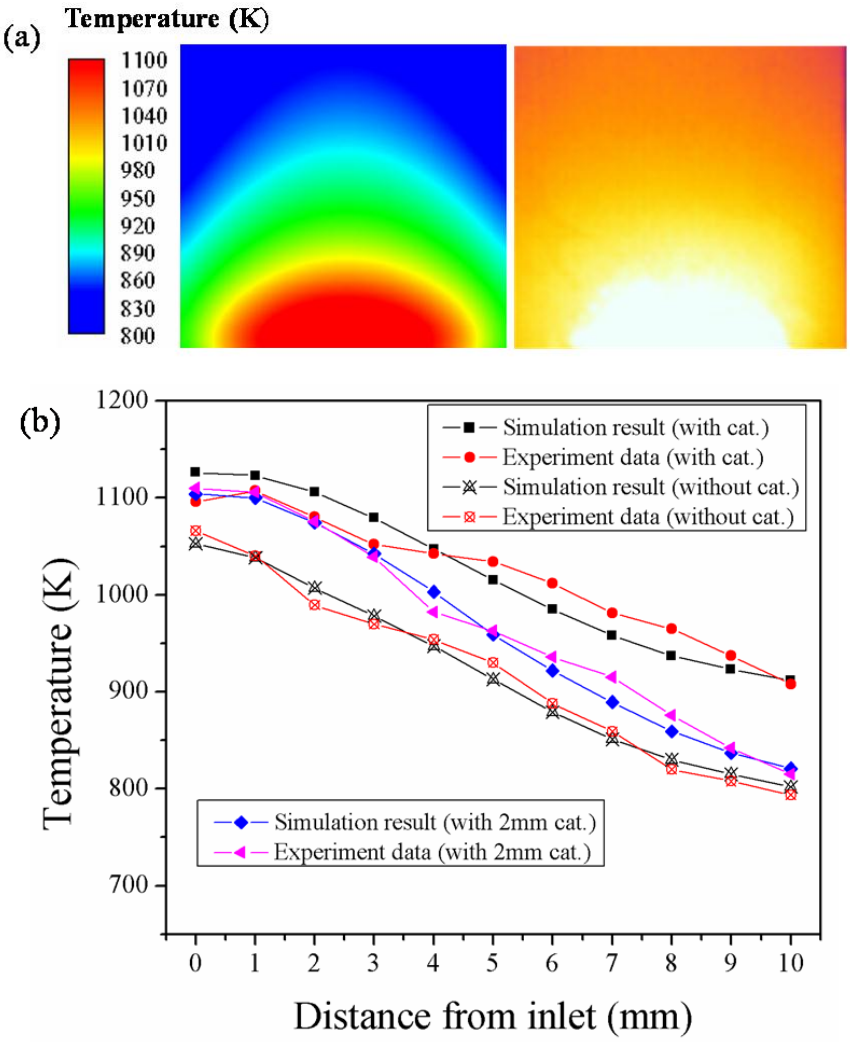

Fig.3. Experimental validation of computational model.(a) Comparison in the outer wall temperature of combustor from simulation and experiment with 2 mm length of catalyst segmentation, (left: simulation; right: experiment), (b) Comparison of centerline temperature profiles on the outer wall of the combustor from experiment and simulation with non-/catalytic wall.

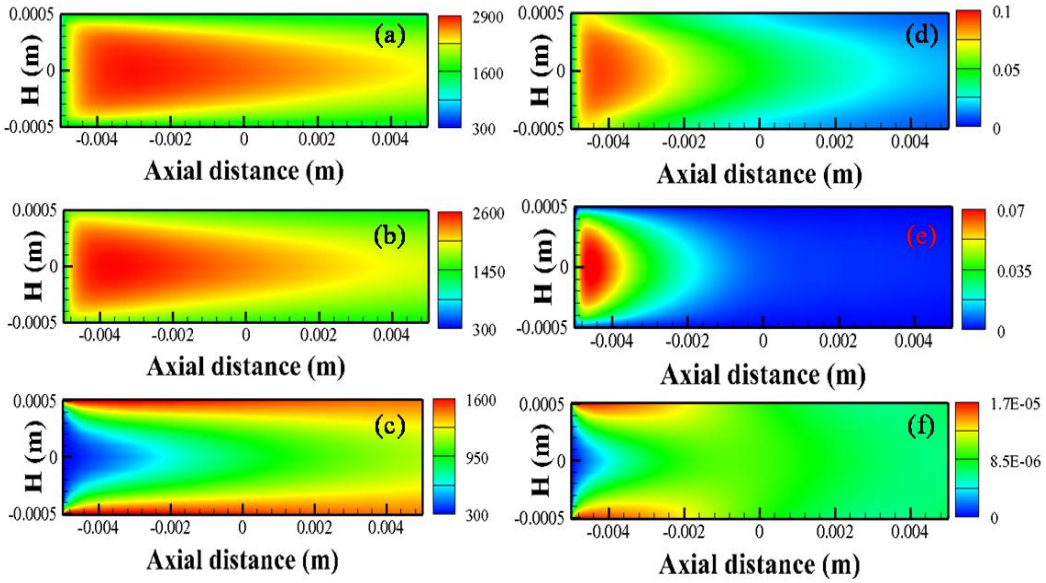

Fig.4.Computed contours of temperature and OH concentration in the center section of micro combustor (y=0) for three cases: (a, d) the Case A, (b, e) the Case B, (c, f) the Case C.

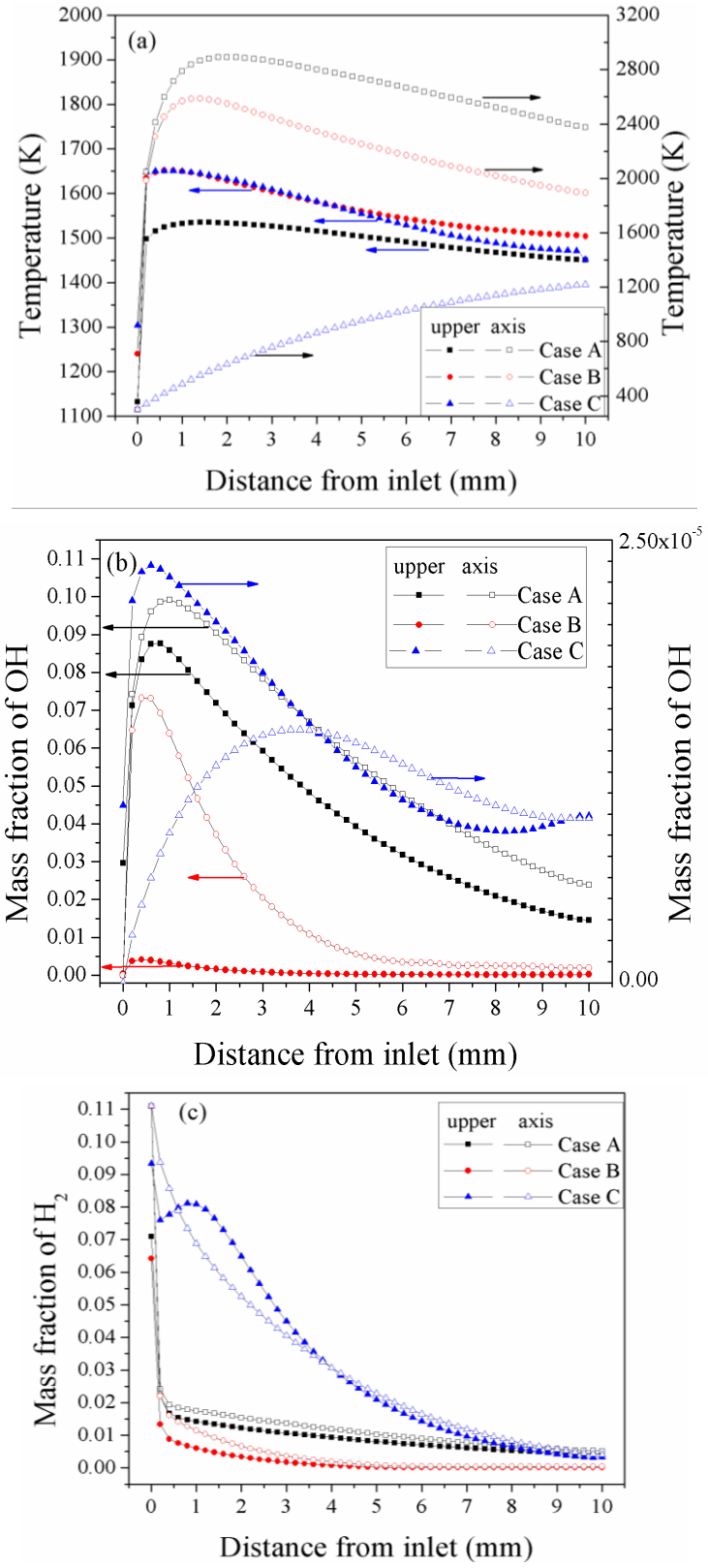

Fig.5. Temperature, OH mass fraction and H_2 mass fraction profiles along the centerline of the flow channel and inner upper wall, (a) temperature profiles, (b) OH mass fraction profiles, (c) H_2 mass fraction profiles.

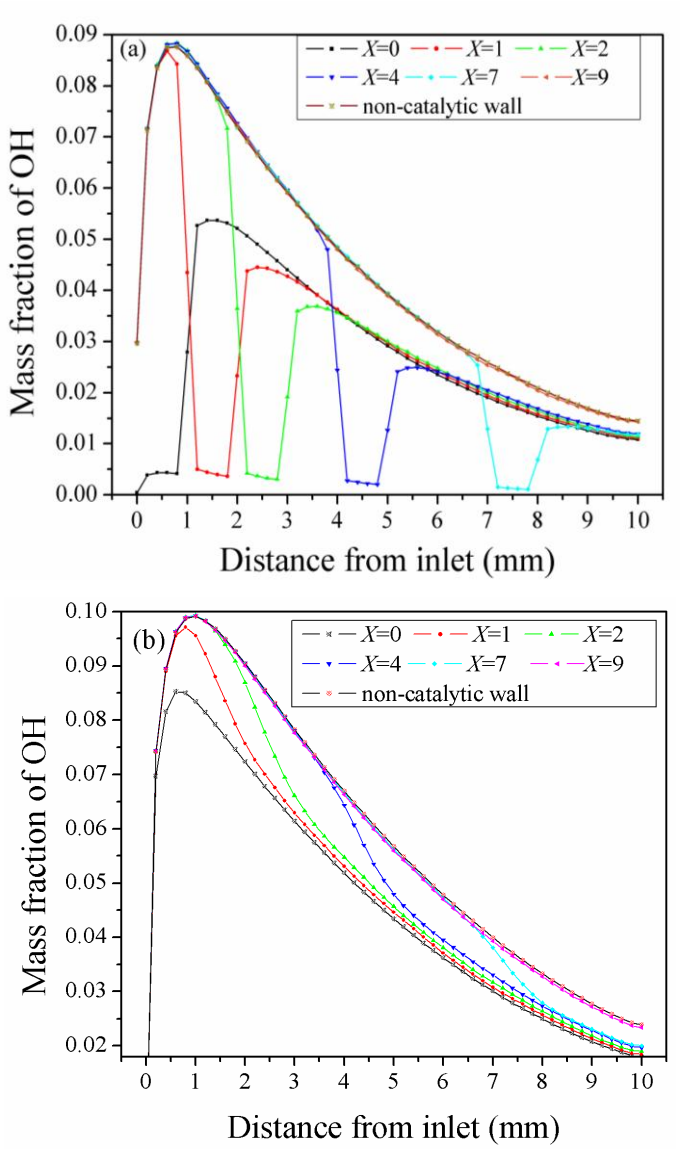

Fig.6. OH mass fraction profiles along the streamwise on the centerline of the inner wall (a) and fluid region (b).

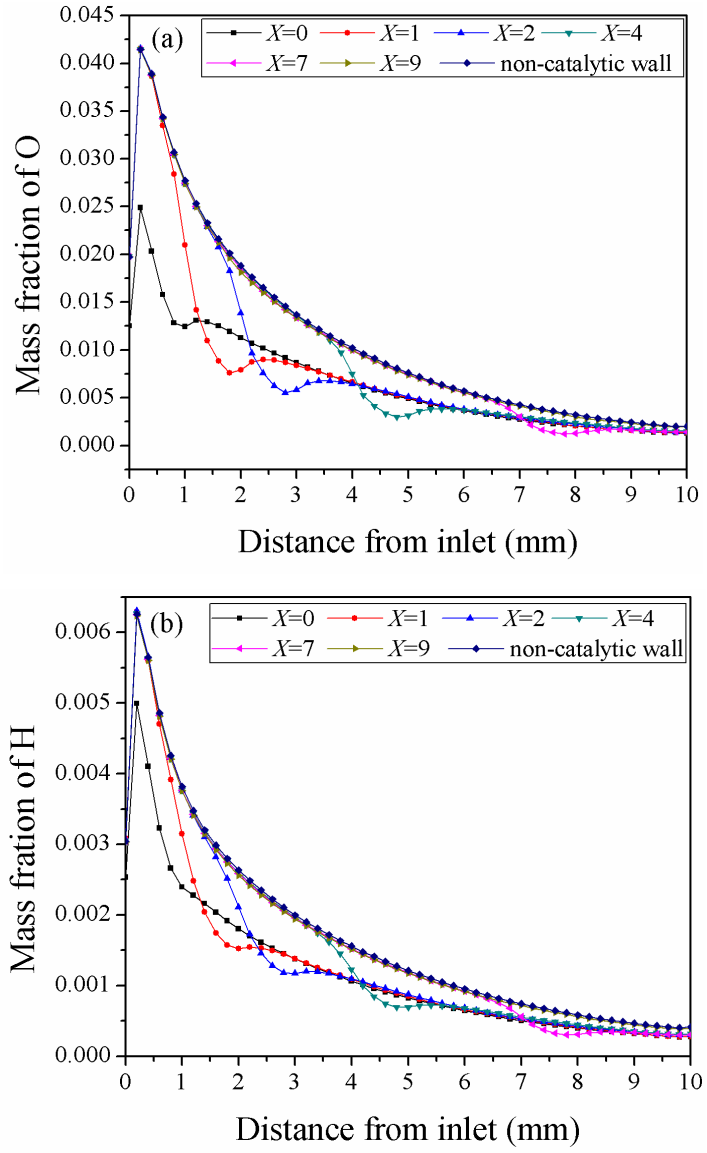

Fig.7. O, H mass fraction profiles on the upper wall along the streamwise, (a) O mass fraction profiles, (b) H mass fraction profiles.

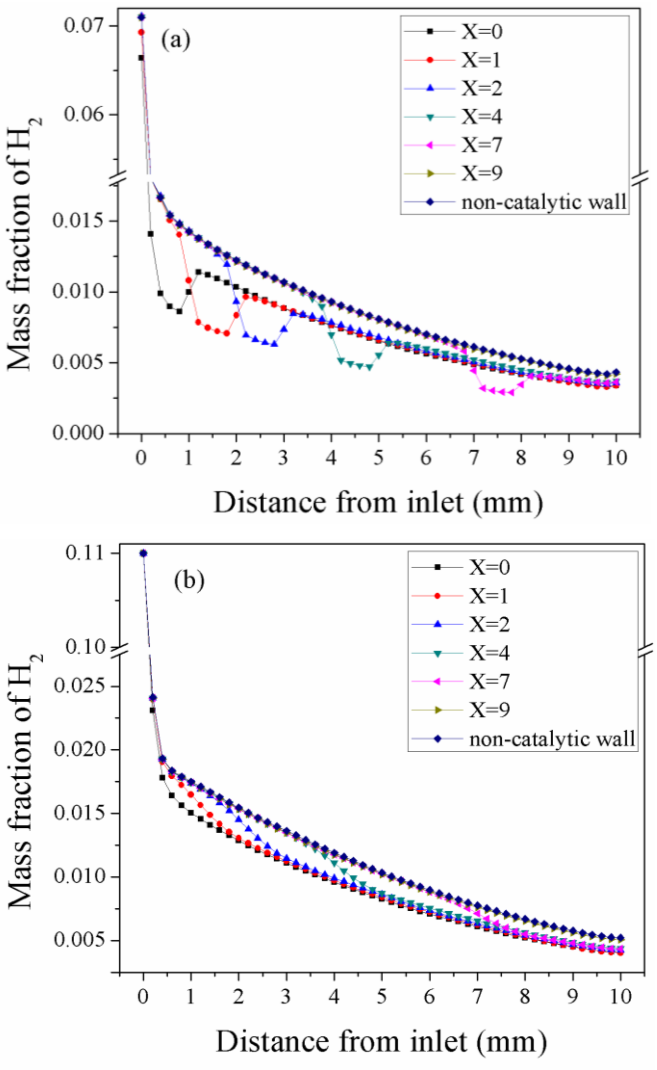

Fig.8. H_2 mass fraction profiles along the streamwise on the centerline of inner upper wall (a) and on the centerline of channel (b).

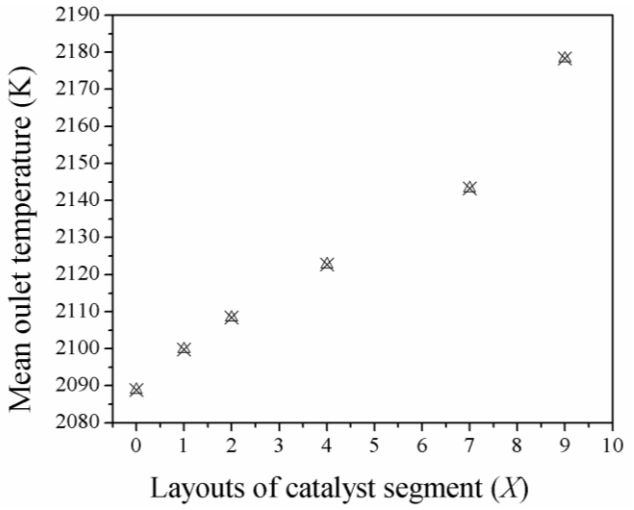

Fig.9. Profile of mean outlet temperature under different positions of catalyst segmentation.

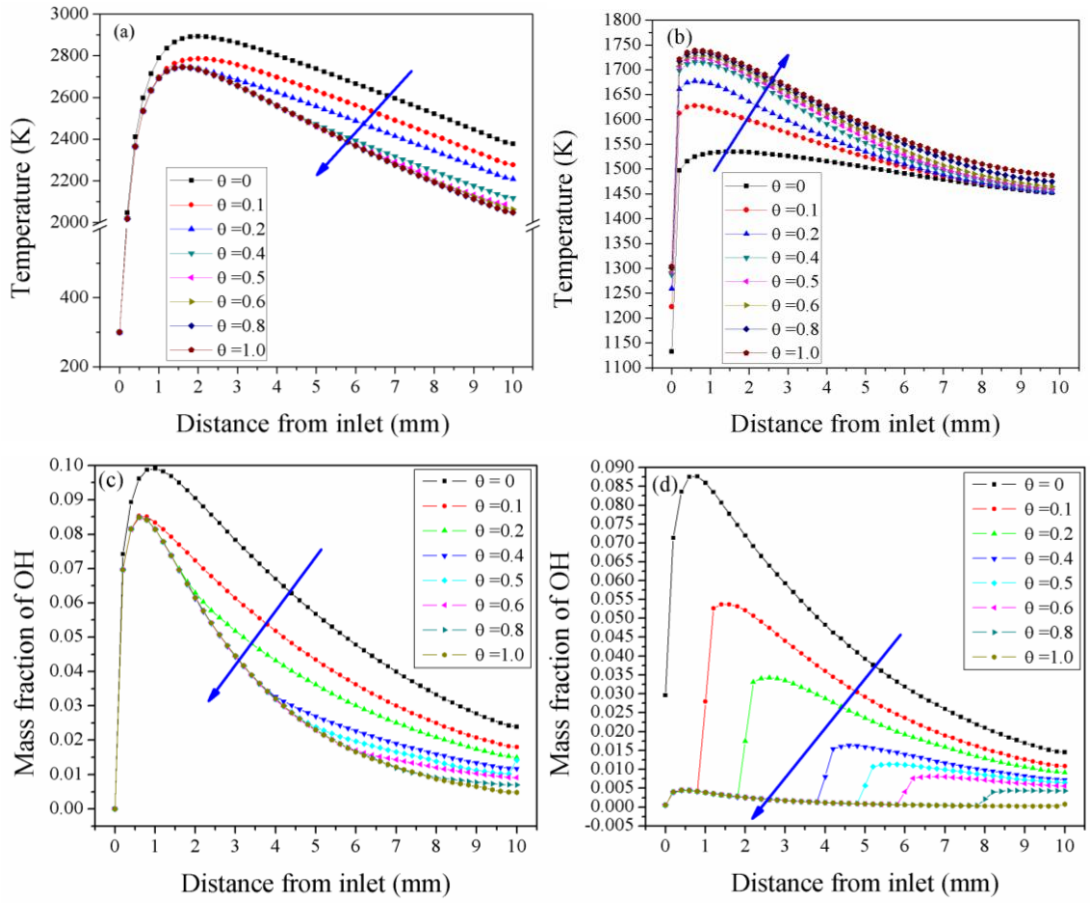

Fig.10. Temperature and OH concentration profiles along the streamwise under different catalytic area ratios: (a) temperature profiles on the centerline of channel, (b) temperature profiles on the centerline of the upper wall, (c) OH concentration profiles on the centerline of channel, (d) OH concentration profiles on the centerline of the upper wall.

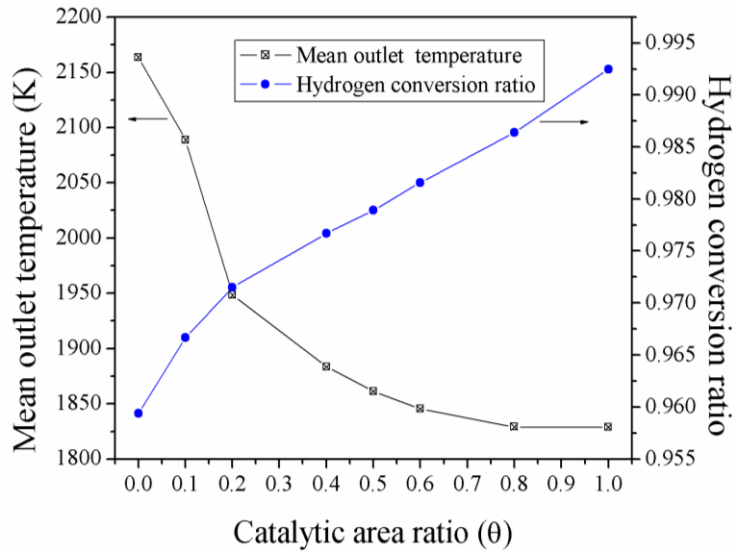

Fig.11. Profiles of mean outlet temperature and hydrogen conversion ratio under different catalytic area ratios.